

Article

# Enhancing Spatial Awareness and Collaboration: A Guide to VR-Ready Survey Data Transformation

Joseph Kevin McDuff, Armin Agha Karimi \* and Zahra Gharineiat 

School of Surveying and Built Environment, University of Southern Queensland, Springfield Central 4300, Australia; w0083590@uemail.usq.edu.au (J.K.M.); zahra.gharineiat@unisq.edu.au (Z.G.)

\* Correspondence: armin.aghakarimi@unisq.edu.au

**Abstract:** Surveying and spatial science are experiencing a paradigm shift from traditional data outputs to more immersive and interactive formats, driven by the rise in Virtual Reality (VR). This study addresses the challenge of transforming UAV (Unmanned Aerial Vehicle)-acquired photogrammetry data into VR-compatible surfaces while preserving the accuracy and quality crucial to professional surveying. The study leverages Blender, an open-source 3D creation tool, to develop a procedural guide for creating VR-ready models from high-quality survey data. The case study focuses on silos located in Yelarbon, Southeast Queensland, Australia. UAV mapping is utilised to gather the data necessary for 3D modelling with a few minor alterations in the photo capturing angle and processing. Key findings reveal that while Blender excels as a visualisation tool, it struggles with geospatial precision, particularly when handling large numbers coming from coordinate systems, leading to rounding errors seen within the VR model. Blender's strength lies in creating immersive experiences for public engagement but is constrained by its lack of capability to hold survey metadata, hindering its applicability for professional survey-grade outputs. The results highlight the need for further development into possible Blender plugins that integrate geospatial accuracy with VR outputs. This study underscores the potential of VR to enhance how survey data are visualised, offering opportunities for future innovations in both the technical and creative aspects of the surveying profession.



Academic Editors: Zhihua Zhang, M. James C. Crabbe and Wolfgang Kainz

Received: 2 December 2024

Revised: 25 January 2025

Accepted: 27 January 2025

Published: 2 February 2025

**Citation:** McDuff, J.K.; Karimi, A.A.; Gharineiat, Z. Enhancing Spatial Awareness and Collaboration: A Guide to VR-Ready Survey Data Transformation. *ISPRS Int. J. Geo-Inf.* **2025**, *14*, 59. <https://doi.org/10.3390/ijgi14020059>

**Copyright:** © 2025 by the authors. Published by MDPI on behalf of the International Society for Photogrammetry and Remote Sensing. Licensee MDPI, Basel, Switzerland. This article is an open access article distributed under the terms and conditions of the Creative Commons Attribution (CC BY) license (<https://creativecommons.org/licenses/by/4.0/>).

**Keywords:** spatial data; drone mapping; virtual reality; Blender; 3D model

## 1. Introduction

In the world of surveying, where traditional data acquisition and presentation techniques have long been the cornerstone of professional practice, new demands are emerging for more interactive and immersive data outputs. Among the most significant technological advancements is Virtual Reality (VR), a tool that offers the potential to revolutionise how survey data are visualised, understood, and communicated. VR provides users with an immersive experience that allows for intuitive navigation through complex spatial data environments, enabling a more detailed exploration of terrains, construction layouts, or topographic survey data [1]. This demand for VR-compatible data poses an important challenge: how can spatial data-collecting professionals (surveyors) ensure that the immersive benefits of VR are achieved without compromising the accuracy, reliability, and quality that are fundamental to the profession?

To understand VR's potential in geospatial areas, it is crucial to grasp its core concept. According to [2], VR involves “inducing targeted behaviour in an organism by using artificial sensory stimulation, while the organism has little or no awareness of the interference”.

This process allows users to experience a designed environment—whether walking, flying, or exploring—through artificially stimulated senses, creating the sensation of being present in an alternate world [3]. As VR technology has evolved, it has become more intuitive and user-friendly, particularly in terms of how users interact with 3D environments [4,5]. The roots of VR, though seen as a contemporary innovation, can be traced back to the late 1980s when companies like Autodesk and VPL first announced VR concepts [6]. Since then, VR has grown to become a tool with enormous potential for various fields, including surveying.

The integration of VR into geospatial and environmental sciences has garnered significant attention in recent years, with numerous studies highlighting its transformative potential. This literature review explores the application of VR in conjunction with advanced surveying technologies such as UAVs, LiDAR, and photogrammetry, as demonstrated in various studies. Ref. [7] exemplifies the application of Immersive Virtual Reality (IVR) in geological mapping. By combining UAV-based Structure-from-Motion (SfM) photogrammetry with Geographic Information System (GIS) analysis, the study achieved high-resolution 3D models for geological features in the Metaxa Mine, Greece. Similarly, [8] demonstrated the transformation of low-altitude UAV imagery into Digital Terrain Models (DTMs) that were subsequently integrated into VR systems. Their findings revealed that VR enhances the user's ability to intuitively explore and analyse spatial terrain in immersive, real-time environments.

In environmental monitoring, ref. [9] compared UAV-based LiDAR and SfM photogrammetry for peatland mapping. They emphasised VR's capability to represent delicate ecosystems with high precision, allowing users to interact with realistic 3D models to better understand hydrological and biogeochemical processes. Papadopoulou and [10] explored the use of LiDAR and VR for flood risk visualisation, demonstrating how geospatial technologies can map flood-prone areas and develop predictive models. Further, ref. [11] highlighted the integration of drones and VR in surface mining, where VR enabled efficient spatial mapping and hazard assessment in high-risk zones.

Furthermore, the commercial construction industry has already recognised the potential of VR [12]. For instance, ref. [13] explored how low-cost VR environments could be used for engineering and construction applications, noting the benefits of combining Building Information Modelling (BIM) with Virtual Reality to enhance visualisation and project planning. Additionally, ref. [14] utilised VR in the context of civil engineering to simulate catastrophic dam failures, integrating UAV photogrammetry with VR technology to communicate disaster risks to the public more effectively. This is highly relevant to surveying, as the construction industry shares similar needs for accurate, geospatially referenced data that can be visualised in 3D environments. The success of VR in these applications suggests that surveyors, too, can benefit from this technology, provided that it is adapted to meet the technical demands of the profession.

These studies collectively underline the versatility and value of VR as a geovisualisation tool in diverse applications, from geological mapping to environmental monitoring and disaster management. By leveraging advanced data collection methods and immersive visualisation capabilities, VR has emerged as a critical component in enhancing spatial awareness, decision-making, and data communication across geospatial disciplines. Surveying, historically confined to traditional outputs such as maps and 2D drawings, now faces the challenge of adapting to these new technological demands. As noted by [15], the surveying profession must continuously evolve to meet societal needs, ensuring that it remains relevant in an increasingly digital and automated world. Surveyors have already expanded their roles beyond cadastral work, incorporating diverse technologies such as UAV photogrammetry and laser scanning. Yet, there remains a significant gap

in the industry to integrate VR-compatible outputs into routine surveying practises. The potential benefits of VR include enhanced spatial awareness, better communication of complex spatial information, and the ability to simulate real-world conditions. However, these advantages can only be realised if the transition to VR does not compromise the core principles of data accuracy and quality assurance inherent in the survey profession.

Unity and Unreal Engine are leading game engines widely used for developing high-fidelity Virtual Reality (VR) applications in geospatial and environmental research. Unity's flexibility, cross-platform compatibility, and ability to integrate 3D models from photogrammetry or LiDAR make it ideal for creating real-time, interactive geovisualisations, as demonstrated by [8] in terrain analysis. Similarly, Unreal Engine offers advanced rendering capabilities and supports the integration of large geospatial datasets, enabling dynamic and visually detailed simulations such as GIS-based environments highlighted by [16]. Both platforms empower users to create immersive VR experiences, enhancing spatial understanding and decision-making across various disciplines.

This research project aims to bridge the gap between traditional surveying outputs and VR-compatible data by leveraging Blender, alongside UAV (Unmanned Aerial Vehicle) photogrammetry data. Blender has been widely used in the media and marketing industries, but its potential as a tool for creating VR environments from high-quality survey data is under-researched. This study seeks to develop a procedural guide that outlines the steps for transforming UAV-acquired photogrammetry data into VR-ready surfaces while maintaining the survey-quality standards expected in the profession. This is performed by creating a five-step process guide that includes data acquisition, modelling, texture shading and lighting, rendering/animation, and finishing with testing and optimisation of VR output.

This study has utilised Blender as the primary platform for preparing VR environments, leveraging its robust capabilities for 3D modelling, texturing, and scene creation. While Blender is a versatile tool with powerful features, its use in VR applications is rarely addressed in the literature. Notable exceptions include studies such as [17], which demonstrated how Blender was employed in archaeological survey projects to create VR environments. Blender, Unity, and Unreal Engine play distinct yet complementary roles in VR development, each excelling in specific areas. Blender serves as a robust platform for creating detailed 3D models, materials, and animations, leveraging its open-source nature and comprehensive toolset to make high-quality asset creation accessible. While Blender focuses on asset preparation, Unity and Unreal Engine are primarily game engines designed for creating interactive, real-time environments. Unity emphasises cross-platform deployment, enabling VR experiences across a wide range of devices, including mobile platforms, making it ideal for accessible, interactive projects. In contrast, Unreal Engine is renowned for its photorealistic rendering capabilities, making it the preferred choice for high-fidelity VR environments in industries like architecture and film. Though Blender allows for the creation of VR-ready assets and provides basic scene preview capabilities, it lacks the tools for real-time interactivity or deployment. Unity and Unreal Engine bridge this gap, offering advanced features such as physics-based simulations, user input, and immersive environment tools, essential for fully interactive VR experiences. Together, these tools form a seamless development pipeline, where Blender's static assets are transformed into dynamic, interactive VR environments through Unity and Unreal Engine.

In addition to developing this VR output format, this study analyses the integrity of survey data when processed through Blender. Specifically, it will address three critical errors that can arise during the VR creation process: height (or relative level) error, horizontal position error, and density error. These errors will be analysed at two key life stages of VR creation: the pre-Blender stage, which is essentially the photogrammetry software stage

(AgiSoft 2.0.2 in this case), and the post-Blender stage, which looks at analysing survey data once imported into Blender. Measurements were conducted between the pre-Blender surface data and the survey data captured on-site using traditional land surveying. This provides a crucial baseline for assessing potential errors before importing the data into Blender. By establishing this baseline, errors introduced by AgiSoft can be effectively isolated from those introduced by Blender during the QA (Quality Assurance) process. Furthermore, it offers a clear gauge of how much the horizontal errors increase after Blender processing, enabling a more precise and comprehensive error analysis.

For example, ref. [17] demonstrated how Blender was employed in archaeological survey projects to create VR environments, enabling detailed 3D reconstructions of historical sites to enhance both public engagement and data preservation efforts.

The broader market for VR is also growing rapidly, with industries ranging from gaming to healthcare investing heavily in the technology [18]. As VR hardware continues to evolve, becoming more accessible and powerful, the demand for VR-ready data will only increase. Surveyors have the opportunity to position themselves at the forefront of this technological shift, offering new services and capabilities that align with the emerging needs of society.

## 2. Materials and Methods

The methodology for transforming standard survey data into VR-compatible outputs follows a five-step process: Data Acquisition/Data Import, Modelling, Texture Shading and Lighting, Rendering/Animation, and Testing and Optimisation. Each step is designed to ensure that the transition from raw survey data to a visually appealing and accurate VR model adheres to industry standards for both data integrity and presentation quality.

### 2.1. Case Study

This research explores the transformation of UAV-acquired photogrammetry data into VR-ready outputs, specifically for surveying applications through a case study that has the complexity to fit the purpose. The chosen site (Figure 1) for this study was GrainCorp's iconic painted silo in Yelarbon ( $28^{\circ}34'16''$  S,  $150^{\circ}45'22''$  E), which is one of many public arts to create the well-known Australian Silo Art Trail. The Yelarbon site, with its challenging vertical structures and stunning artwork (titled: "When the Rain Comes"), provided a unique and visually engaging subject for testing this VR transformation process. Grain-Corps expressed interest in utilising the VR output to validate VR's relevance in surveying while supporting a cultural and marketing initiative.



**Figure 1.** The Yelarbon silo art—'When the Rain Comes', (GrainCorp owned).

## 2.2. Data Acquisition

The data acquisition process for this project (Figure 2) relied on UAV photogrammetry, which allows for the efficient capture of high-resolution imagery and 3D data from the air [19]. The UAV used for this project was the DJI Phantom 4 PRO v2.0, a widely recognised commercial-grade drone in the surveying industry (Figure 2). Its 1-inch, 20 MP camera and mechanical shutter make it ideal for capturing detailed textures and large structures like the Yelarbon silos without introducing image distortion.



**Figure 2.** Images from the fieldwork for the project and the drone utilised for data collection.

For stationary objects like the Yelarbon silos, the camera settings were optimised to capture intricate details clearly and with minimal noise. The settings used were ISO 100, f/5.6, and a 1/400 shutter speed (further details in Table 1). This combination ensured that the camera could capture the silo artwork in high detail at various angles without overexposure or motion blur. The drone was operated in shutter priority mode, allowing automatic adjustments to aperture and ISO to maintain consistent exposure throughout the flight. These camera settings allowed us to capture high-quality images that served as the basis for photogrammetric modelling in later stages.

**Table 1.** Camera and flight properties used in the data collection of the study.

Property	Value
Camera model	FC6310S
F-stop	f/5.6
Exposure time	1/320 s
ISO speed	ISO-100
Exposure bias	0 step
Focal length	9 mm
Max aperture	2.97
Height range (AHD)	170–220 m
Study area mean height (AHD)	160 m
Pitch range	0°–80°

Given the vertical nature of the silos, a combination of two UAV flight patterns was employed: a linear flight plan for nadir image acquisition and a circular flight for oblique image acquisition. The linear flight plan was designed to capture the entire area with the camera orientated directly downward (nadir), ensuring overall coverage of the site. The circular flight plan, on the other hand, was essential for capturing the silo's vertical surfaces and detailed textures from multiple angles [20]. This flight plan significantly reduced occlusions and allowed for a more comprehensive 3D model of the structure by integrating data from both horizontal and vertical aspects. The use of these two flight paths ensured that the UAV achieved the necessary 60% image overlap for effective photogrammetric reconstruction, particularly important for vertical structures like the Yelarbon silos, which stand over 10 m tall. The camera settings for the Yelarbon silos survey were meticulously planned to capture VR-ready outputs, considering the site's ground RL of 160 m and silo heights of 180–190 m. The shooting plan ensured comprehensive coverage with top-down (nadir) and oblique imagery (Figure 3). Most photos (51.95%) were taken at 220 m altitude with a 0° pitch for complete site coverage, while detailed oblique images were captured at 180 m and 190 m. A significant portion (25.13%) of images had a 60° pitch to capture angled surfaces. The plan also accounted for optimal lighting, high overlap, and multi-angle imagery to enhance texture detail and minimise artefacts, ensuring accurate and aesthetically pleasing VR-ready models.

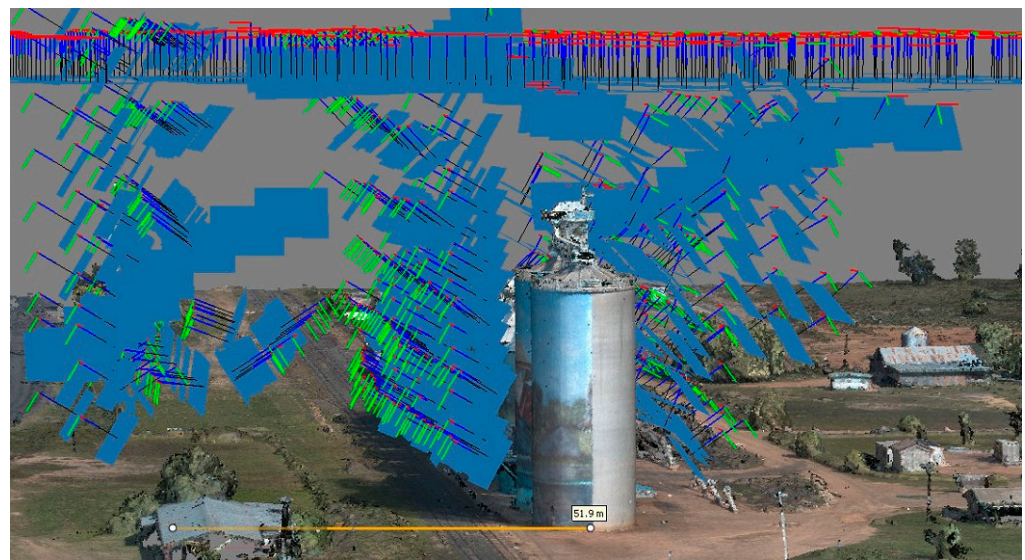


**Figure 3.** Drone data capture trajectory. The side view is chosen to highlight oblique view data collection.

Ground Control Points (GCPs) are critical for georeferencing the photogrammetric data, ensuring that the final model is accurate in scale and location. The coordinate system used in this study is the Map Grid of Australia 2020 (MGA2020) Zone 56. For this site, seven GCPs were placed around the site, as shown in Figure 4, providing a reliable spatial framework and an aesthetically pleasing model without warping, scale distortion, misalignment, or artefacts. The local Permanent Survey Marks (PSMs) are used to reference the GCP and spot height checks; later these spot heights are used to verify the accuracy of not only the Agisoft-generated surface model but also test for distortions from Blender.



**Figure 4.** Oblique imagery of the Yelarbon Silo, highlighting the project case study location, including GCP, PSM, and Rico Pictures utilised for both photogrammetry and land surveying data collection.

### 2.3. Image Processing in AgiSoft

This study utilises AgiSoft, a photogrammetric software capable of processing images from RGB or multispectral cameras into high-value spatial information, such as georeferenced photogrammetric point clouds and textured polygonal models. The software ensures that the resulting Digital Surface Models (DSMs) and Digital Terrain Models (DTMs) maintain georeferencing throughout the modelling process. For image processing, the generic settings in AgiSoft were adopted. Specifically, the ‘Align Photos’ parameters were set at 40,000 key points and 4000 tie points.

The generation of 3D representations from processed images was achieved through point cloud generation. The process involved the following steps:

1. Pixel iteration: Each pixel in the image was examined individually.
2. 3D location calculation: The three-dimensional location of each pixel was calculated, projecting it from the image plane.
3. Trigonometric calculations: Trigonometry was employed to determine the spatial position, using basic angles and triangles.
4. View ray identification: Each pixel was treated as a point along a line originating from the camera (the “view ray”).
5. Intersection with image plane: The intersection of the view ray with the image plane represented the pixel’s location in 3D space.
6. 3D coordinate calculation: Once the intersection point was determined, the 3D coordinates of each pixel were computed in either real-world units or relative to the image plane’s dimensions.

Upon generating the point cloud, surface reconstruction was performed. The DEM was created using Inverse Distance Weighting (IDW), a photogrammetric interpolation method that estimates elevation values based on surrounding known points. In this method, geotagged image coordinates are used to interpolate the positions of unknown points, with

closer points having more influence on the estimation. IDW was selected due to its superior performance around structures, ensuring precise elevation modelling.

The following settings were adopted for texture generation as the output progressed to the Blender stage:

- Texture Type: Diffuse Map, Occlusion Map
- Source Data: Images, 3D Model (high quality: 4.7 settings)
- Mapping Mode: Generic, Orthophoto, Adaptive Orthophoto, Single Camera, Keep UV
- Blending Mode: Mosaic (default), Average, Max Intensity, Min Intensity, Disabled
- Texture Size/Count:  $4096 \times 1$
- Advanced Options: Enable Hole Filling, Enable Ghosting Filter

Once the surface model was complete, it was exported as an OBJ file, a standard format for 3D models that includes the data vertices, edges, faces, and textures. The texture images were extracted as JPEGs, which Blender uses to apply realistic surface textures to the 3D model. These formats ensured a smooth transition from AgiSoft to Blender (version 4.0), with minimal loss of detail or data integrity.

#### 2.4. Modelling in Blender

The overall Blender workflow is presented in Figure 5. With the OBJ file and textures imported into Blender, the next steps involved refining the model to prepare it for rendering and VR output. The imported model was primarily manipulated using Object Mode, which allowed adjustments to the silo's position, scale, and rotation within the virtual environment. Object Mode was chosen due to its versatility in handling overall transformations of the model.

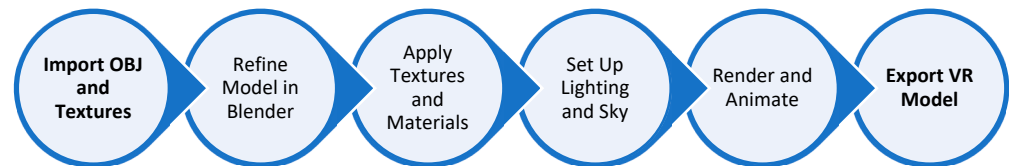


**Figure 5.** Workflow for modelling VR in Blender.

Blender models are composed of three basic elements: vertices, edges, and faces (Figure 6a). Vertices represent individual points in 3D space, edges connect two vertices, and faces are the visible surface formed by three or more edges. These geometric components were modified where necessary to ensure the model's structure was accurate and free of defects that could affect the final rendering.

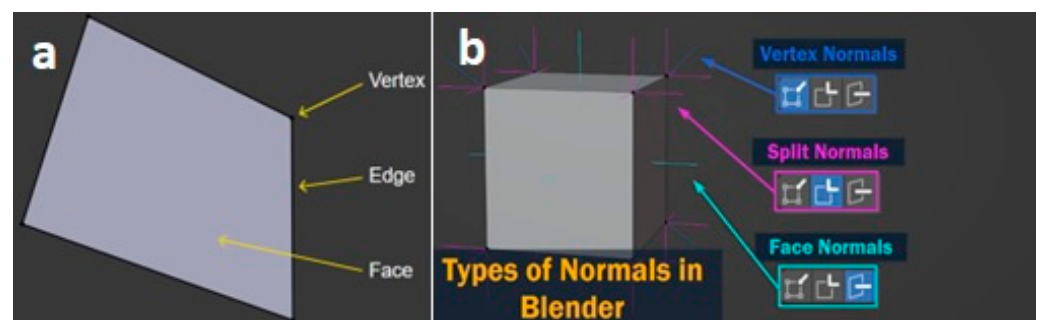


**Figure 6.** (a) Blender basic elements, (b) Blender normals with different variations, such as split normals, which separate normals for each selected vertex, and vertex normals, which are 3D coordinates representing lines that are perpendicular to the model's surface geometry.

Unlike traditional CAD programs, Blender treats each face as independent. This required careful inspection to prevent unintended gaps or inconsistencies. One of the important considerations when working with 3D meshes in Blender is normals (Figure 6b). Normals defines the direction of the faces and help the software differentiate between the inside and outside of the mesh. Given that Blender is not inherently spatially aware (e.g., in terms of North, East, or West), correctly orienting the normals was necessary to avoid rendering issues.

Blender's Viewport Shading Modes (Figure 7) are utilised throughout the modelling process to visualise the structure at different stages. These modes are Wireframe Mode, Solid Mode, and Rendered Display Mode, which help assess and refine the model. By utilising these modes, the model was fine-tuned and optimised for seamless integration into the VR environment, ensuring that the textures and geometry would display correctly during the rendering process.

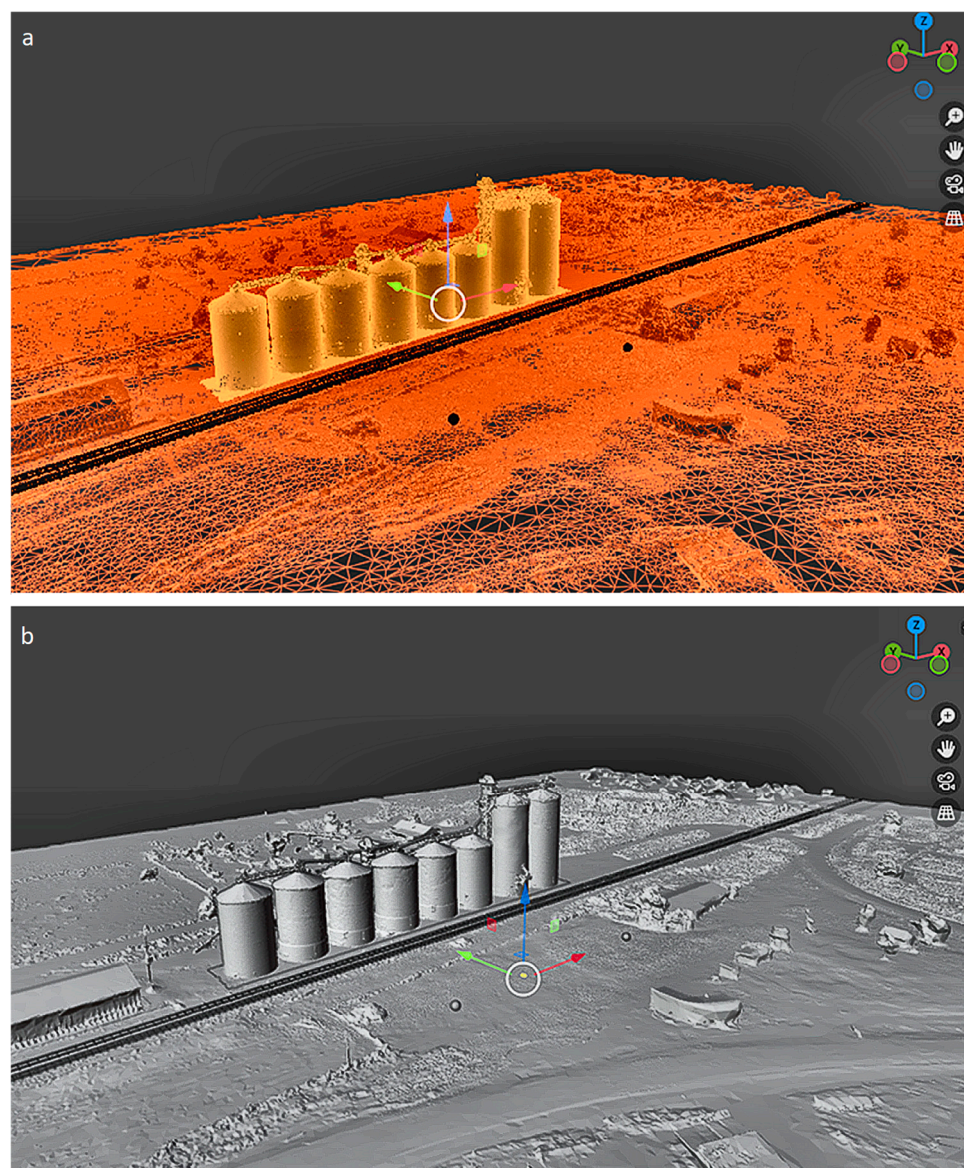


Figure 7. Cont.



**Figure 7.** Blender’s Viewport Shading Modes: (a) Wireframe Mode provides a clear view of the model’s underlying geometry, allowing for an inspection of the vertex and edge structures. (b) Solid Mode displays the model’s surface without textures, aiding in the identification of any geometric inconsistencies. (c) Rendered Display Mode gives a preview of the textured model, allowing us to evaluate texture alignment, lighting, and other visual elements before final rendering.

Applying textures and materials to 3D models in Blender enhances their visual appeal and realism. Additionally, lighting plays a key role in creating realistic effects. Before delving into texture application and lighting for the Yelarbon Silo VR project, it is crucial to understand how nodes function in Blender, as they control both texture and lighting elements. In particular, it is required to distinguish between the Principled BSDF (Bidirectional Scattering Distribution Function) and Blender nodes.

The Principled BSDF is a simplified node that manages the creation of materials in Blender. It is a physically based shader that combines multiple shader types into a single node, which forms the core of material creation in Blender. Other nodes serve as modular blocks that contain structured data, transforming inputs into outputs based on predefined parameters. These nodes are organised visually in Blender as an interconnected tree structure (Figure 8).

Through these nodes, the modeller can interact with light and textures. Blender supports two main texture types: image textures (photos or graphics) and procedural textures (mathematically generated patterns). This project exclusively focuses on image textures created from UAV photogrammetry for the Yelarbon Silo.

The Principled BSDF combines multiple material layers into a single, easy-to-use node. It can simulate a wide variety of materials, as demonstrated in Figure 9a, where different material properties such as diffuse, subsurface, metallic, and transmission are applied using the same base colour. This node is fundamental in setting up realistic textures for the VR model.

Blender’s metallic property allows materials to transition between a dielectric look and a metallic finish. A metallic value of 0.0 indicates a material with a diffuse or transmissive base layer, topped by a specular reflection. A value of 1.0 results in a fully specular material that reflects the base colour without diffuse reflection (Figure 9b).

In the Yelarbon Silo art, increasing the metallic value made surfaces appear shinier and more reflective, enhancing the sense of realism. This effect highlighted how light interacts with the silo surface, creating bright highlights and deep shadows that emphasise the silo’s contours. By adjusting the metallic properties, attention was drawn to specific areas,

such as the eight silos, creating visual contrast and emphasising qualities like strength and precision.

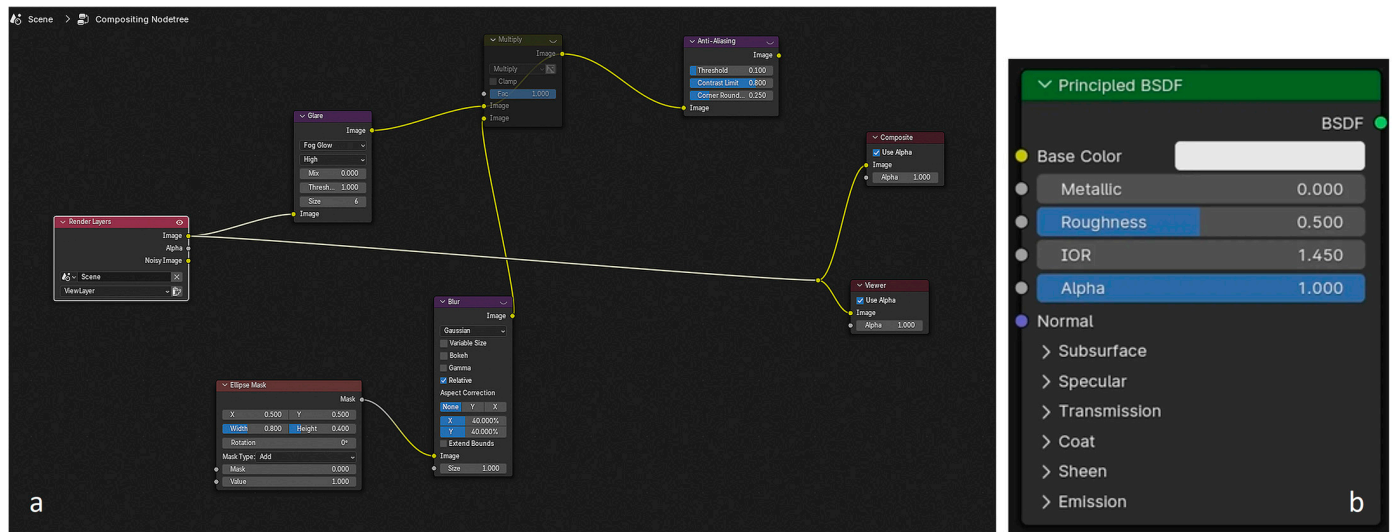


**Figure 8.** (a) Blender nodes connected to the Principled BSDF to create texture effects for the model. (b) Principled BSDF is a shader node that combines multiple layers into one to model a variety of materials.

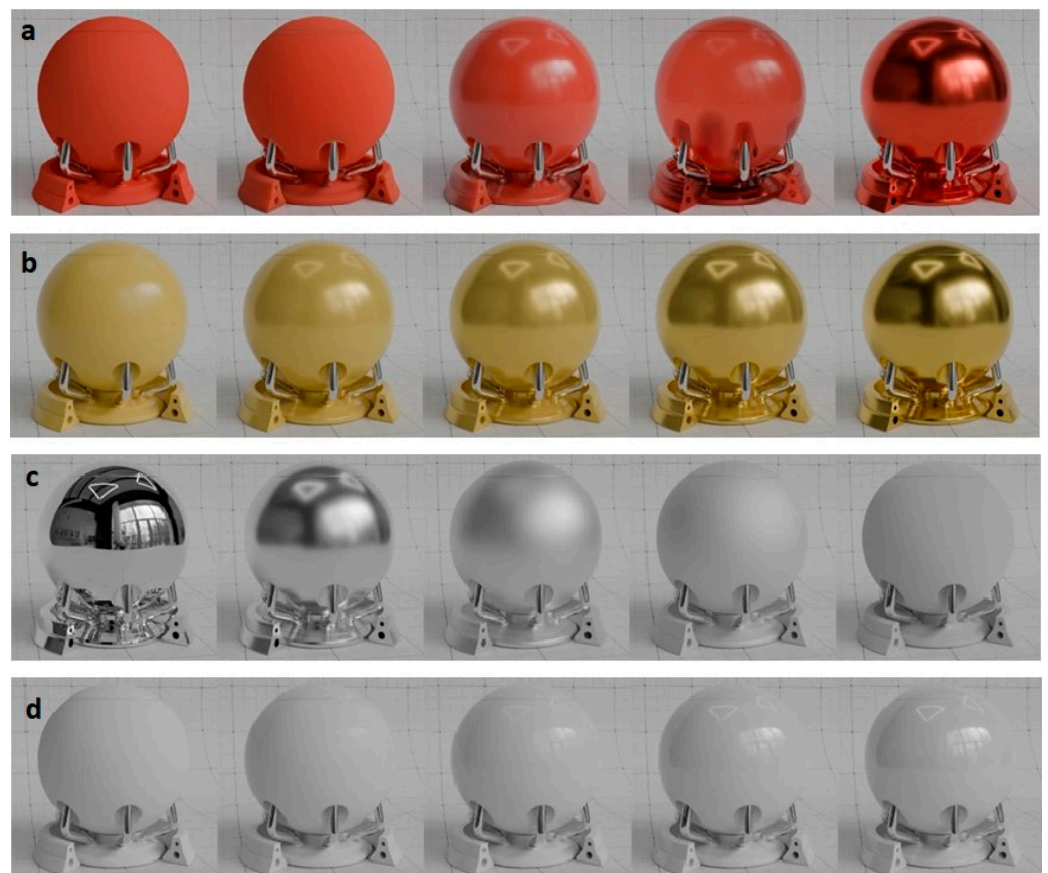


**Figure 9.** (a) The Principled BSDF demonstrating the effects of mixing texture values such as subsurface, metallic, and transmission (b) metallic properties from values of 0 to 1.0, (c) roughness properties from values of 0 to 1.0, and (d) index of refraction Properties from values of 0 to 1.0.

The roughness setting specifies the microfacet roughness of a surface, affecting specular reflection and transmission (Figure 9c). For the Yelarbon Silo art, increasing the roughness added texture and depth, giving the silo a more tactile, realistic feel. Higher roughness values emphasise material details, such as wood grain or fabric texture, enhancing the viewer's perception of the surface. This can convey a sense of ruggedness or authenticity, making the object appear more worn or natural.

The Index of Refraction (IOR) depicts how light bends through transparent materials like glass or water. While IOR is not extensively used in this specific journal's surface model, it is important to note that for most materials, the IOR typically ranges between 1.0 (vacuum or air) and 4.0 (germanium). The default value of 1.5 in Blender approximates glass (Figure 9d).

The Hue/Saturation/Value (HSV) Node applies colour transformations using the HSV colour model. Adjusting saturation, in particular, can make textures appear more vibrant or stylised, enhancing their visual impact. In the Yelarbon Silo project, the initial model appeared dull and lifeless due to overexposure from the sun and the limitations of the 1-inch 20 MP CMOS camera used (Phantom 4 Pro 2). The current settings for the Principled BSDF showed a saturation value of 0 and a value of 1, resulting in a flat appearance. By increasing the saturation to 5 and adjusting the value to 0.9, the texture's vibrancy became noticeably improved (Figure 10). In a related example from a Blender tutorial, lowering the saturation produced a black-and-white effect, creating a more sombre scene. This approach, similar to the greyscale aesthetics seen in Yelarbon Silo art, reduced the saturation while keeping the value at 1, achieving a more pronounced, dramatic effect.



(a)



(b)

**Figure 10.** (a) Higher colour saturation model at a saturation value of 5 and a value of 0.9; (b) more natural saturation mode with a saturation value of 0 and a value of 1.

The Sky Texture Node adds a procedural sky texture to the VR model, enriching its visual depth and realism. By enhancing features like clouds, gradients, and atmospheric effects, the sky contributes to the mood of the scene. A well-textured sky can evoke different emotions, from calmness with soft clouds to tension with darker stormy formations. This serves as a striking backdrop, complementing the silo and other elements within the model.

The Sun Elevation setting controls the angle of the sun above the horizon, significantly influencing the scene's lighting and mood. Lower sun elevations, such as during sunrise or sunset, cast longer shadows and create warm, golden light, adding depth and drama to the scene. A midday sun, with a higher elevation, produces shorter, more direct shadows and a neutral lighting effect. The choice of sun elevation was crucial in determining the time of day and overall visual tone for the Yelarbon Silo art project.

Sun Rotation refers to the sun's movement around the zenith, altering the direction and length of shadows throughout the day. Morning and evening light, known as "golden hours", provide soft, warm tones with long shadows, enhancing textures and depth. The midday sun, being directly overhead, creates harsher lighting and shorter shadows, resulting in a flatter appearance. Adjusting the sun's rotation allowed us to simulate different times of day, affecting the lighting mood of the VR environment.

### *2.5. Rendering and Animation in Blender*

Rendering, in its most basic form, involves capturing multiple panoramic images and compiling them into a seamless video, which creates the illusion of continuous footage. Watching 24 frames per second (fps) is a typical industry standard and one that this study adopts. This approach is essential for creating VR content, where fluidity and immersion are critical to the viewer's experience. With the Silo model's texture and lighting all taken care of, rendering the process can be broken down into three key Blender properties: Camera Object Data, Render Settings, and Output Properties. These settings allow for the fine-tuning of how the final VR environment is captured, rendered, and exported. The Camera Object Data Properties in Blender are essential for simulating realistic camera effects, controlling how scenes are captured, and optimising them for VR environments. The camera is the lens through which the rendered world is viewed, though it remains invisible in the final render. The lens type dictates how 3D objects are represented in a 2D image. The perspective lens option, which mimics human vision, was chosen for this project. Objects farther from the camera appear smaller, and parallel lines converge at a distance, giving a sense of depth that is critical for VR experiences.

The focal length controls how much of the scene is visible in the frame. A shorter focal length allows a wider field of view (FOV), capturing more of the environment, which is essential for VR to enhance the user's immersive experience. Conversely, a longer focal length narrows the FOV, which is less desirable for panoramic content creation. For this project, a focal length optimised for a broad FOV was selected to provide the most immersive experience possible in VR. An equirectangular projection was used to create a full 360° panoramic render of the scene. This type of projection is critical for VR, as it renders an environment map compatible with world shaders in Blender, making it possible to view the entire scene from any angle. The camera was aligned to the positive X axis to ensure accurate projection mapping. The render properties in Blender determine the output quality of the images and animations generated. As cameras are invisible in renders, material or texture settings were not needed for the camera itself. Instead, focus was placed on selecting the appropriate rendering engine and optimising the render settings to ensure high-quality outputs with minimal artefacts.

The Cycles render engine was chosen for its physically accurate simulation of lighting, reflections, and shadows. These qualities are essential for creating realistic VR content,

where the sense of immersion hinges on believable lighting conditions. Cycles utilises Path Tracing, which calculates light interactions within the scene to achieve these effects. To expedite the rendering process, GPU rendering was employed. Modern GPUs are highly efficient at handling the complex computations required for rendering, significantly reducing the time needed to produce each frame. However, GPU rendering has its limitations, particularly regarding memory usage. The project was carefully managed to ensure that the available GPU memory was not exceeded during the rendering of the complex VR environment. Another key consideration was the Noise Threshold, which was adjusted to minimise artefacts in the rendered images. A higher threshold results in fewer imperfections at the cost of longer rendering times. For this project, a balance was struck between rendering time and image quality to produce the cleanest possible output without unnecessarily prolonging the process.

Render samples directly impact the quality of the final image. Higher sample rates result in better quality but also increase rendering time. The Integrator, which is responsible for simulating light paths, was fine-tuned to maximise the realism of reflections and shadows in the VR environment. The settings were optimised to strike a balance between high-quality output and efficient rendering times. The output properties determine how the final render or animation is exported, impacting both its performance and appearance in VR.

The frame range was set to ensure that the final animation consisted of 24 frames per second (fps), the industry standard for VR content and video playback. This ensured smooth transitions between frames and a natural viewing experience for the user. The resolution was set to  $1920 \times 1080$  pixels (Full HD), balancing visual quality with manageable file size and rendering time. Although higher resolutions such as 4K ( $3840 \times 2160$  pixels) could have been used, Full HD was selected to maintain efficient rendering times without sacrificing too much visual clarity. A frame rate of 24 fps was chosen, as this is the standard for most VR and cinematic content. The frame rate ensures smooth playback while keeping the file size manageable. Blender allows for custom frame rates, but for this project, 24 fps was optimal for both technical and practical reasons.

The final product of the case study can be found at the following link: <https://www.youtube.com/watch?v=eEntVHeFNv8> (accessed 31 January 2025).

### 3. Quality Testing

In addition to transforming UAV-acquired photogrammetric data into VR-compatible outputs using AgiSoft and Blender, this study also aimed to address a secondary objective: evaluating the quality of spatial data and identifying errors when processed through AgiSoft and Blender. The focus was on dimensional and positional errors as well as the density error. These errors were evaluated at two distinct stages:

1. In the photogrammetric model: The photogrammetric surface created in AgiSoft is compared to exact precise survey data obtained using conventional land surveying. It should be noted that a third party, Maptrek Point Studio, was used for comparison.
2. In the VR model: After importing the photogrammetric model into Blender, the dimensional, positional, and density metrics were re-evaluated using Blender's internal measurement tools. Two types of coordinate systems were considered:
  - Shifted coordinate system: The photogrammetric model was shifted to Blender's Cartesian system.
  - Reference coordinate system: The photogrammetric model retained its original geospatial coordinates in MGA2020 Zone 56, allowing us to recognise distortions introduced by Blender.

To systematically analyse the errors, quartiles and descriptive statistics are used in all error categories. Quartiles (Figure 11) divide a dataset into four equal parts, providing a detailed summary of how the errors are distributed across different measurements [21]. Thanks to quartiles, it is possible to determine the central tendency (median, Q2), assess the spread of the data (Q1, Q3), and identify outliers by analysing the lower and upper fences.

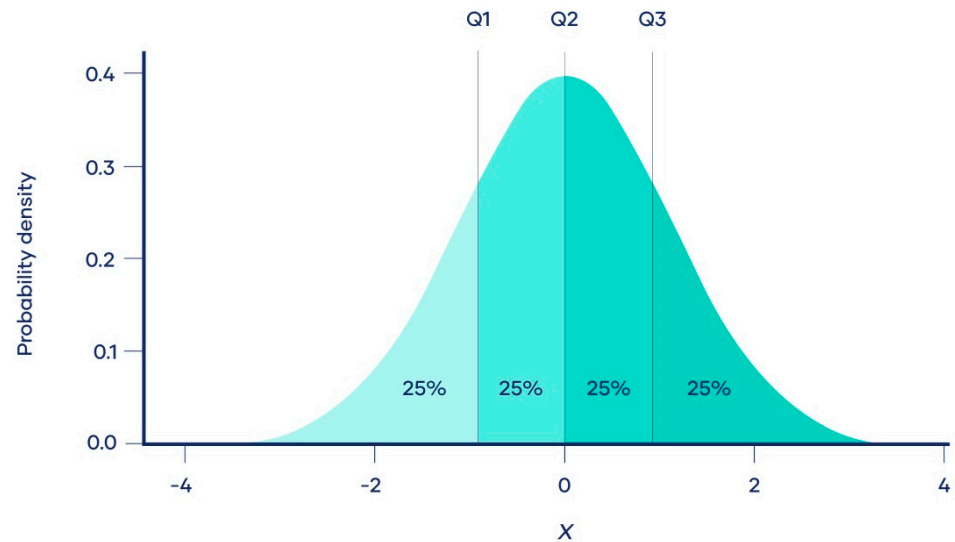


**Figure 11.** Quartiles split the data into four parts with an equal number of observations. Source: <https://www.scribbr.com/statistics/quartiles-quantiles/> (accessed 31 January 2025).

Figure 12 shows the photogrammetric model with baseline spheres created in Maptrek Point Studio, which are used as references to identify potential deformities during data processing in Blender. It also presents high-precision land surveying measurements and the silo sphere measurements from eight silos, demonstrating how Blender maintains the relative alignment and surface integrity of the silos after import.

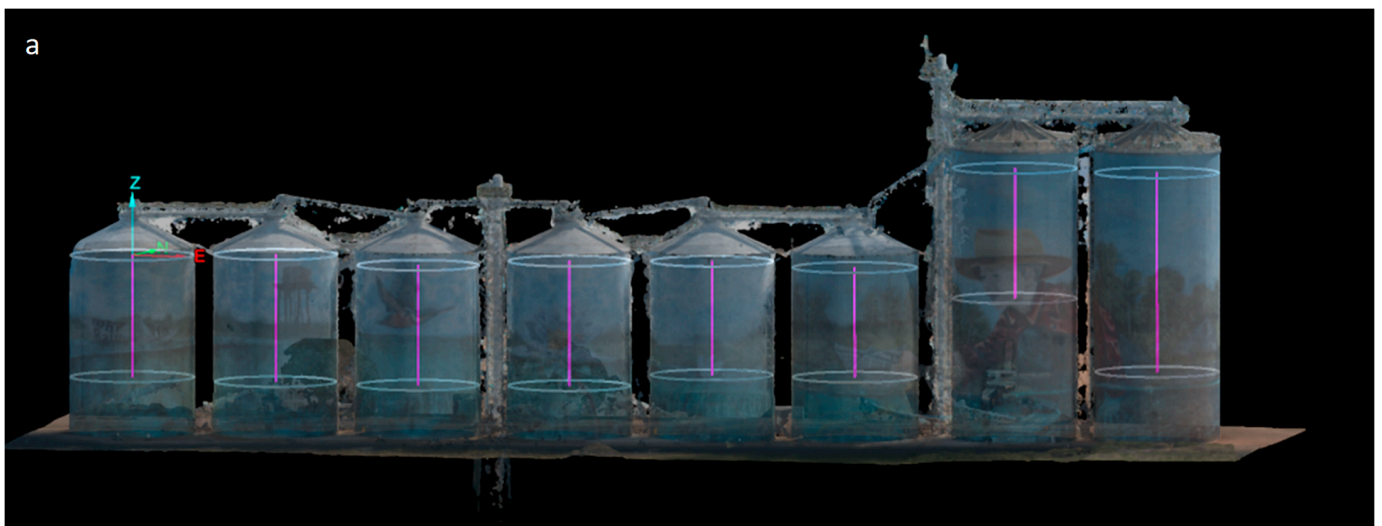


**Figure 12.** *Cont.*

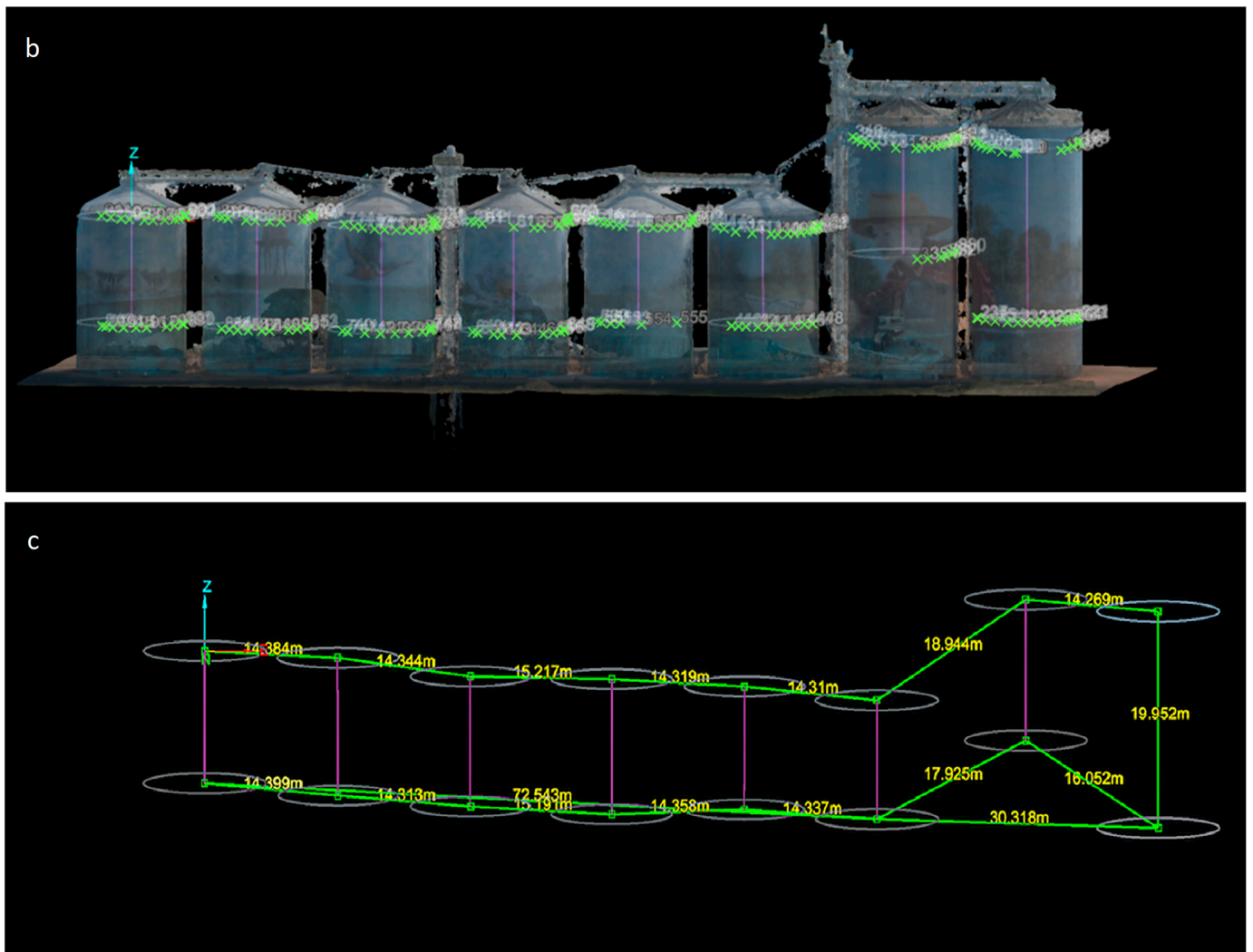


**Figure 12.** (a) The photogrammetric model with baseline spheres created in Maptek Point Studio. These silo spheres act as essential references for identifying potential deformities introduced during data processing in Blender. The baseline measurements from Maptek provide a crucial comparison point to validate the accuracy of the Agisoft-generated surfaces when transformed within Blender's coordinate system. (b) High-precision measurements obtained by land surveying. (c) The silo sphere measurements from each of the eight silos. These measurements are used to determine whether Blender maintains the relative alignment and surface integrity of the silos after being imported.

After importing the photogrammetric model into Blender, the errors were re-evaluated, revealing that Blender introduced a distortion related to decimal precision. This issue arose because Blender's Cartesian coordinate system struggled with large real-world values, such as those in the MGA2020 coordinate system, which includes high easting and northing values. Blender's handling of large spatial coordinates led to a loss of decimal precision, particularly with values beyond the typical X, Y, and Z scale range. This precision loss distorted the model, significantly affecting the accuracy of the imported data. This distortion is observed in the results before and after Blender processing, shown in Figure 13.

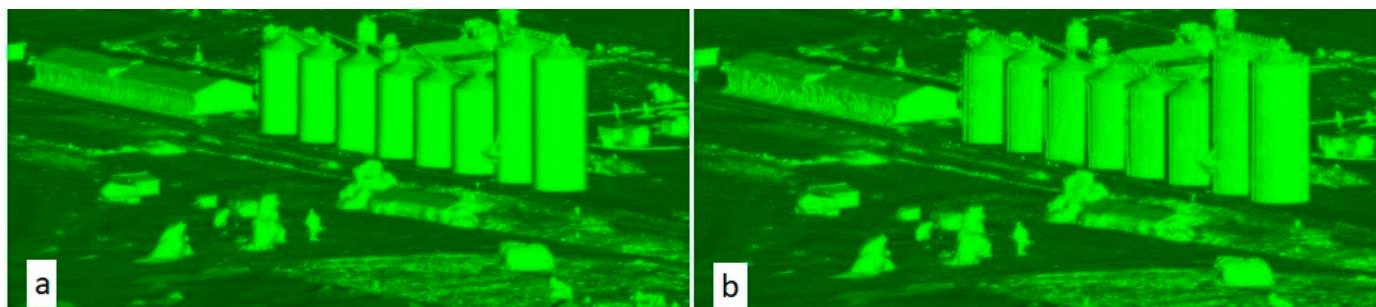


**Figure 13.** (a) The photogrammetric model, which shows no distortion, and (b) the VR model that has visible distortions.

### 3.1. Dimensional and Positional Error

First, the horizontal accuracy of the photogrammetric model compared to precise survey data is evaluated, and then further analyses are carried out on the impact of processing these data in Blender. The goal of this analysis is to examine how well Blender maintains the spatial integrity of the model, specifically the radius, enclosed area, total edge length, and mesh surface of the silos when processing geospatial data.

Table 2 shows the statistical parameters of the accuracy reached in the photogrammetric model. The radius differences reveal that the photogrammetric model typically underestimates the radius compared to survey data, with minor discrepancies overall but some significant outliers. These differences can largely be attributed to the precision and accuracy of silo capture in traditional surveying. For enclosed areas, the photogrammetric model tends to record smaller values than survey data, with median differences around  $-4.72 \text{ m}^2$  and a lower fence of  $-34.92 \text{ m}^2$  indicating substantial deviation in some of the data from the expected range or trend. In terms of total edge length, the photogrammetric model generally underestimates when compared to survey data, with a median difference of  $-0.78 \text{ m}$ . However, there are instances where the photogrammetric model has longer lengths. The precision in capturing silo edges during the survey contributes significantly to these differences.

**Table 2.** Photogrammetric model error statistics.

	Radius (m)	Enclosed Area (Best Fit Plane) ( $\text{m}^2$ )	Total Edge Length (m)	Easting Diff.	Northing Diff.	RL Diff.	Mesh Surface Difference (Upper)	Mesh Surface Difference (Lower)
Average	-0.096	-3.194	-0.568	0.123	-0.106	0.185	0	-0.012
Quartile 1	-0.326	-12.058	-2.005	0.018	-0.389	-0.003	-0.226	-0.237
Quartile 2	-0.095	-4.723	-0.775	0.127	-0.098	0.077	-0.019	-0.024
Quartile 3	0.010	3.179	0.515	0.358	0.202	0.340	0.227	0.205
Lower Fence	-0.830	-34.916	-5.785	-0.491	-1.277	-0.519	-0.907	-0.901
Upper Fence	0.178	10.798	1.775	0.527	0.498	0.512	0.454	0.426

Table 3 compares statistical metrics between the VR model (in local coordinates) and the photogrammetric model, indicating a high degree of consistency between the two software tools. The radius difference has an average of  $-0.007 \text{ m}$ , suggesting a negligible reduction in the VR model's measurements compared to the photogrammetric model. Quartiles and fences around zero show that these differences are minor, with no significant outliers, indicating consistent radius measurements across both models.

**Table 3.** VR model (shifted coordinates of the photogrammetric model) error statistics.

	Radius (m)	Enclosed Area (Best Fit Plane) (m <sup>2</sup> )	Total Edge Length (m)	Easting Diff.	Northing Diff.	RL Diff	Mesh Surface Difference (Upper)	Mesh Surface Difference (Lower)
Average	−0.007	−0.027	0.055	N/A	N/A	N/A	0.075	−0.029
Quartile 1	0.000	−0.002	0.036	N/A	N/A	N/A	−0.001	0
Quartile 2	0.000	0.000	0.073	N/A	N/A	N/A	0.001	0
Quartile 3	0.000	0.001	0.114	N/A	N/A	N/A	0.226	0.001
Lower Fence	−0.001	−0.007	−0.081	N/A	N/A	N/A	−0.340	−0.001
Upper Fence	0.001	0.002	0.153	N/A	N/A	N/A	0.340	0.001

For the enclosed area, there is a slight average decrease of  $-0.027 \text{ m}^2$  in the VR model relative to the photogrammetric model. The distribution of values around zero, with low variability, suggests that both tools are almost identical in calculating area, with only minor discrepancies. The total edge length has an average positive difference of  $0.055 \text{ m}$ , showing a small increase in Blender's edge length measurements. The range from  $-0.081 \text{ m}$  to  $0.153 \text{ m}$  implies some variation but remains modest, suggesting that the edge length is generally well-aligned between the VR model and the photogrammetric model. The Easting, Northing, and RL differences are not applicable here, due to the shift, so no horizontal discrepancies are reported between the models on these axes. For the mesh surface differences, the upper surface shows a slight positive difference ( $0.075 \text{ m}$ ), and the lower surface has a small negative difference ( $-0.029 \text{ m}$ ). This suggests that the VR model has a slightly elevated upper surface and a somewhat deeper lower boundary compared to the photogrammetric model. While the overall variability in the upper surface is minimal, the lower and upper fences ( $\pm 0.340 \text{ m}$ ) indicate the presence of a few points where the VR model's upper surface deviates more significantly from the photogrammetric model. These outliers, although limited in number, reflect localised discrepancies in the surface alignments.

Table 4 provides the statistical metrics for the VR model in which the coordinates have not been shifted, revealing mostly minor discrepancies across several dimensions. For the radius, there is a slight average difference of  $-0.033 \text{ m}$ , indicating that the VR model's radius measurements tend to be marginally smaller than the photogrammetric model. The enclosed area shows an average increase of  $0.3 \text{ m}^2$  in Blender's model, with the values distributed around zero, suggesting slight variability. In terms of total edge length, the average difference is minimal at  $0.017 \text{ m}$ , though the range of values indicates some variation in edge lengths, with some segments appearing shorter in Blender and others slightly longer. When looking at Easting and Northing differences, Easting shows a small average deviation of  $0.028 \text{ m}$ , with a more significant range on the lower side. Northing, however, shows no observable difference, suggesting consistency between the models along this axis.

The vertical difference remains zero across all measurements, indicating that while the easting and northing coordinates are affected by decimal errors, the RL values are not impacted and remain consistent to the fourth decimal place. The mesh surface differences reveal that both the upper and lower surfaces exhibit similar discrepancies, suggesting that the decimal error is not localised to higher x-values but rather affects the entire model uniformly.

**Table 4.** VR model (original coordinates of the photogrammetric model) error statistics.

	Radius (m)	Enclosed Area (Best Fit Plane) (m <sup>2</sup> )	Total Edge Length (m)	Easting Diff.	Northing Diff.	RL Diff	Mesh Surface Difference (Upper)	Mesh Surface Difference (Lower)
Average	−0.033	0.300	N/A	0.018	0.029	0	−0.454	−0.465
Quartile 1	−0.071	−0.212	N/A	−0.205	−0.265	0	−0.646	−0.631
Quartile 2	0	0.192	N/A	−0.017	0.008	0	−0.193	−0.190
Quartile 3	0	0.347	N/A	0.309	0.286	0	0.601	0.555
Lower Fence	−0.178	−1.051	N/A	−0.978	−1.090	0	−2.518	−2.410
Upper Fence	0.036	0.627	N/A	0.567	0.561	0	1.225	1.149

### 3.2. Density Error

While it has been observed that Blender modifies the spatial positioning, specifically the easting and northing coordinates, its impact from a model density perspective is yet to be determined. Upon comparing vertices, edges, faces, and triangles between the data exported from AgiSoft and that processed in Blender, no discrepancies are found. This consistency indicates that the structure of the 3D model remains faithful to the original survey data, which is crucial for surveying projects where any change in density could affect the model's spatial accuracy.

## 4. Discussion

This section focuses on an evaluation of the methodology for spatial analysts to create VR-ready outputs based on UAV survey-quality data alongside a discussion on the error results obtained from the VR model. The study follows five key steps in data transformation and error assessment, addressing two critical questions: how can this process be achieved, and can Blender—primarily an artistic tool—deliver the precision needed for surveying outputs despite its non-geospatial design?

The first step relied on robust UAV survey practises, primarily using nadir and oblique photogrammetry for data capture. Oblique imagery was particularly important, as noted by [20], due to the vertical structure of the Yelarbon silos. This method ensured that the silo's surfaces were adequately captured in both horizontal and vertical aspects, allowing for more accurate and immersive VR experiences. One key challenge identified in this step was the balance between media-quality image textures and survey-grade data integrity. Although photogrammetry inherently allows for detailed texture mapping, the methodology had to accommodate oblique images for vertical structures like silos, which are less common in standard surveying practice. The additional use of GCPs and image overlap helped mitigate errors in surface accuracy. This step illustrates the intersection between traditional surveying techniques and the requirements for creating VR-compatible output.

In terms of 3D modelling, Blender demonstrated strong capabilities for surface manipulation and mesh handling, with the vertices and point cloud density generally being well-preserved. However, the core distinction between Blender and traditional survey software became clear: Blender is primarily built for artistic purposes, not geospatial accuracy. Blender handles Cartesian coordinates efficiently, but it struggles with geographic coordinates and lacks the tools needed to perform map projections or geospatial transformations. This limitation became particularly evident when working with real-world Easting and Northing coordinates, as seen in the Yelarbon silo dataset. Due to the practical constraints of importing only .obj files, Blender was unable to accurately retain essential metadata,

such as coordinate system information (in this case, the MGA2020 Zone 56 dataset), surface attributes, break lines, and survey annotations or metadata tags. These deficiencies highlight that, although Blender excels in visualisation and modelling, it is not fully equipped for tasks where geospatial precision is critical.

The texture shading and lighting processes in Blender proved to be an area where spatial analysts would face the most significant learning curve. Despite having strong spatial awareness and 3D understanding, surveyors may find it challenging to navigate Blender's UV mapping, shader editor, and material properties. The technical aspects of UV mapping, in particular, can be difficult for survey professionals unfamiliar with node-based workflows, which involve manipulating properties like colour, roughness, and transparency to achieve realistic textures. Moreover, lighting plays a critical role in the final presentation of VR environments, as different light types (e.g., Point, Sun, Area) can dramatically alter the appearance of textures.

Rendering and animation are where Blender's limitations in survey applications became most evident. Blender offers two main rendering engines—Eevee for fast, real-time rendering and Cycles for high-quality, physically accurate renders. The importance of sample adjustments for noise reduction, file format selection, or video rendering settings needs to be considered, and they make it difficult to export VR content effectively. Render resolution is another important factor. Surveyors accustomed to technical precision need to be appreciated for output resolution to be (e.g., 1080p for HD video) when creating VR content for platforms like YouTube. Furthermore, file management, especially for large video files, can pose logistical challenges, especially for those not familiar with managing render files and post-processing workflows.

The introduction of the photogrammetric model to Blender was immediately met with problems, mostly due to decimal handling issues when real-world geospatial coordinates give Blender some red in its ledger. Due to poorly handling big coordinate values, Blender causes distortion when inputting the photogrammetric model to create the VR model. It should be noted that additional research was performed on these decimal error findings consistent with issues reported by some users on Blender Stack Exchange, where users noted similar distortions when importing large coordinate systems. To address these challenges, subsequent tests focused on correcting horizontal errors by realigning the model to local coordinates (e.g., 0X, 0Y, 0Z) in an effort to reduce the distortions introduced during the import process.

After realigning the surface to Blender's local coordinate system, the comparison between the VR model and the photogrammetric model indicated that Blender maintained a high level of consistency. The average radius deviation was minimal, suggesting that Blender's local coordinate system can retain the geometric fidelity of imported models with negligible distortion. The enclosed area differences were also minor. This demonstrates Blender's ability to preserve spatial integrity when realignment is applied, effectively mitigating distortions that could otherwise impact the accuracy of the final model. Easting and northing comparisons showed uniform errors across all sections of the model. In this case, the error was confined to the decimal places of the coordinates. The RL (vertical) differences were minimal and remained consistent throughout the analysis, suggesting that while the easting and northing coordinates experienced decimal-level errors, the RL values were less impacted.

The observed errors in this study can be attributed to a combination of data acquisition, processing, and conversion. During data acquisition, the quality of UAV imagery plays a pivotal role in ensuring the fidelity of the photogrammetric model. While nadir imagery is essential for capturing horizontal surfaces, oblique imagery proved critical for reconstructing vertical structures like the Yelarbon silos. Suboptimal flight paths or insufficient image

overlap could lead to incomplete data capture, introducing gaps or inaccuracies in surface reconstruction. To reduce errors and enhance model accuracy and quality, several measures are recommended: 1. Using extra GCPs, particularly on the silos. 2. Further optimising UAV flight paths by increasing image overlap and incorporating additional oblique captures to improve data completeness and minimise gaps; and 3. Utilising higher-resolution cameras with enhanced dynamic range to reduce noise and improve texture detail.

A comparison of the model's density (vertices, edges, faces, and triangles) before and after Blender processing showed no changes, suggesting that while Blender distorted horizontal and height data, it preserved the overall model structure. This consistency is essential for ensuring that the visual and structural fidelity of survey outputs remains intact during transformations.

Testing Blender's capability to model the silo in terms of radius, enclosed area, and total edge length provided critical insights; however, the quality of the silo capture during the survey was significantly impacted. Discrepancies and outliers compared to the survey data made a comprehensive assessment challenging. Would this level of error align with LaValle's concept of virtual presence [2]? Despite these errors, would it still manage to "fool" a user into feeling immersed in a virtual environment? Or would higher-quality capture be necessary? Is relying solely on UAV data causing the VR concept data to be ineffective before it even reaches Blender? It is difficult to definitively determine the model's accuracy in creating a sense of presence.

## 5. Conclusions

This study underscores Blender's potential as a robust visualisation tool for creating immersive, VR-compatible models that excel in stakeholder engagement, marketing, and public education. Its ability to preserve the structural density and visual fidelity of 3D models highlights its utility in applications where visualisation quality is paramount. However, Blender's current limitations, particularly in handling large real-world coordinate systems and ensuring geospatial accuracy, restrict its adoption for professional survey-grade applications.

Addressing these limitations requires targeted improvements. Developing external plugins or tools to support map projections and real-world geospatial coordinates in Blender could significantly enhance its precision. Furthermore, integrating Blender with professional software like BIM (Building Information Modelling) and GIS (Geographic Information Systems) would create a comprehensive workflow, combining Blender's visualisation strengths with the analytical rigour of these specialised tools. This integration would broaden Blender's applicability across industries such as civil engineering, where it could simulate construction workflows, and archaeology, where it could enhance digital reconstructions for public engagement and preservation.

To verify the feasibility and effectiveness of these proposed solutions, applying the research findings to practical projects would be essential. This could involve testing Blender in real-world scenarios, such as creating VR environments for urban planning or disaster management, where both visualisation quality and data accuracy are critical. Such efforts would provide valuable insights into Blender's capabilities and limitations, informing its evolution as a reliable tool in professional applications.

In conclusion, while Blender currently faces challenges in achieving the geospatial precision required for survey-grade applications, its potential to modernise how survey data are visualised and understood is significant. By addressing its limitations and exploring its integration with advanced technologies and software, Blender could play a transformative role in the future of VR modelling and geospatial visualisation across a wide range of professional fields.

**Author Contributions:** Conceptualization, Joseph Kevin McDuff; methodology, Joseph Kevin McDuff, Armin Agha Karimi, Zahra Gharineiat; software, Joseph Kevin McDuff; validation, Joseph Kevin McDuff; formal analysis, Joseph Kevin McDuff; investigation, Joseph Kevin McDuff; resources, Joseph Kevin McDuff, Armin Agha Karimi; data curation, Joseph Kevin McDuff; writing—original draft preparation, Joseph Kevin McDuff; writing—review and editing, Armin Agha Karimi, Zahra Gharineiat; visualisation, Joseph Kevin McDuff; supervision, Armin Agha Karimi; project administration, Joseph Kevin McDuff. All authors have read and agreed to the published version of the manuscript.

**Funding:** This research received no external funding.

**Data Availability Statement:** The raw data supporting the conclusions of this article will be made available by the authors on request.

**Acknowledgments:** We would like to thank GrainCorp for their cooperation in letting us collect the data. We also thank the anonymous reviewers for their constructive comments.

**Conflicts of Interest:** The authors declare no conflicts of interest.

## References

- Langer, E. *Media Innovations AR and VR: Success Factors for the Development of Experiences*; Springer Nature: Berlin/Heidelberg, Germany, 2023.
- LaValle, S.M. *Virtual Reality*; Cambridge University Press: Cambridge, UK, 2023.
- Boulos, M.N.K.; Lu, Z.; Guerrero, P.; Jennett, C.; Steed, A. *From Urban Planning and Emergency Training to Pokémon Go: Applications of Virtual Reality GIS (VRGIS) and Augmented Reality GIS (ARGIS) in Personal, Public and Environmental Health*; Springer: Berlin/Heidelberg, Germany, 2017; Volume 16, pp. 1–11.
- Faust, N.L. The virtual reality of GIS. *Environ. Plan. B Plan. Des.* **1995**, *22*, 257–268. [[CrossRef](#)]
- Haklay, M.E. Virtual reality and GIS: Applications, trends and directions. In *Virtual Reality in Geography*; CRC Press: Boca Raton, FL, USA, 2001; pp. 59–69.
- Chesher, C. Colonizing virtual reality: Construction of the discourse of virtual reality. *Cultronix* **1994**, *1*, 1–27.
- Antoniou, V.; Bonali, F.L.; Nomikou, P.; Tibaldi, A.; Melissinos, P.; Mariotto, F.P.; Vitello, F.R.; Krokos, M.; Whitworth, M. Integrating Virtual Reality and GIS Tools for Geological Mapping, Data Collection and Analysis: An Example from the Metaxa Mine, Santorini (Greece). *Appl. Sci.* **2020**, *10*, 8317. [[CrossRef](#)]
- Halik, Ł.; Smaczyński, M. Geovisualisation of relief in a virtual reality system on the basis of low-level aerial imagery. *Pure Appl. Geophys.* **2018**, *175*, 3209–3221. [[CrossRef](#)]
- Kalacska, M.; Arroyo-Mora, J.P.; Lucanus, O. Comparing UAS LiDAR and Structure-from-Motion Photogrammetry for peatland mapping and virtual reality (VR) visualization. *Drones* **2021**, *5*, 36. [[CrossRef](#)]
- Papadopoulou, E.E.; Papakonstantinou, A. Combining Drone LiDAR and Virtual Reality Geovisualizations towards a Cartographic Approach to Visualize Flooding Scenarios. *Drones* **2024**, *8*, 398. [[CrossRef](#)]
- Singh, P.; Murthy, V.; Kumar, D.; Raval, S. A comprehensive review on application of drone, virtual reality and augmented reality with their application in dragline excavation monitoring in surface mines. *Geomat. Nat. Hazards Risk* **2024**, *15*, 2327399. [[CrossRef](#)]
- Ahmed, S. A review on using opportunities of augmented reality and virtual reality in construction project management. *Organ. Technol. Manag. Constr. Int. J.* **2018**, *10*, 1839–1852. [[CrossRef](#)]
- Hilfert, T.; König, M. Low-cost virtual reality environment for engineering and construction. *Vis. Eng.* **2016**, *4*, 2. [[CrossRef](#)]
- Spero, H.R.; Vazquez-Lopez, I.; Miller, K.; Joshaghani, R.; Cutchin, S.; Enterkine, J. Drones, virtual reality, and modeling: Communicating catastrophic dam failure. *Int. J. Digit. Earth* **2022**, *15*, 585–605. [[CrossRef](#)]
- Hannigan, B. The role of surveying in society—Has it changed? *Aust. Surv.* **1990**, *35*, 209–228. [[CrossRef](#)]
- Pavelka, K., Jr.; Landa, M. Using Virtual and Augmented Reality with GIS Data. *ISPRS Int. J. Geo-Inf.* **2024**, *13*, 241. [[CrossRef](#)]
- Montagnetti, R.; Mandolesi, L. QGIS, pyarchinit and blender: Surveying and Management of Archaeological data with Open Source Solutions. *Archeomatica* **2019**, *10*. [[CrossRef](#)]
- Raji, M.A.; Olodo, H.B.; Oke, T.T.; Addy, W.A.; Ofodile, O.C.; Oyewole, A.T. Business strategies in virtual reality: A review of market opportunities and consumer experience. *Int. J. Manag. Entrep. Res.* **2024**, *6*, 722–736. [[CrossRef](#)]
- Kim, S.J.; Jeong, Y.; Park, S.; Ryu, K.; Oh, G. A survey of drone use for entertainment and AVR (augmented and virtual reality). *Augment. Real. Virtual Real. Empower. Hum. Place Bus.* **2018**, 339–352. [[CrossRef](#)]

20. Aicardi, I.; Chiabrandò, F.; Grasso, N.; Lingua, A.M.; Noardo, F.; Spanò, A. UAV photogrammetry with oblique images: First analysis on data acquisition and processing. *Int. Arch. Photogramm. Remote Sens. Spat. Inf. Sci.* **2016**, *41*, 835–842. [[CrossRef](#)]
21. Altman, D.G.; Bland, J.M. Statistics notes: Quartiles, quintiles, centiles, and other quantiles. *BMJ* **1994**, *309*, 996. [[CrossRef](#)] [[PubMed](#)]

**Disclaimer/Publisher’s Note:** The statements, opinions and data contained in all publications are solely those of the individual author(s) and contributor(s) and not of MDPI and/or the editor(s). MDPI and/or the editor(s) disclaim responsibility for any injury to people or property resulting from any ideas, methods, instructions or products referred to in the content.